ELSEVIER

Journal of Chromatography A, 906 (2001) 417–442

JOURNAL OF CHROMATOGRAPHY A

www.elsevier.com/locate/chroma

Review

Atomistic modeling of enantioselection in chromatography

Kenny B. Lipkowitz*

Department of Chemistry, Indiana University–Purdue University at Indianapolis, 402 N. Blackford Street, Indianapolis, IN 46202, USA

Abstract

A review of atomistic molecular modeling studies related to chromatographic separations of enantiomers is presented. Only those types of calculations where direct interactions between a selector and a selectand are involved are described in this review; omitted are regression models. An emphasis is placed on comparing methods used for sampling potential energy surfaces implementing different methodologies like quantum and molecular mechanics for energy calculations, and molecular dynamics and Monte Carlo sampling strategies for simulations. Type I–V chiral stationary phases and additives for capillary electrophoresis and ion-pair chromatography are covered in this review. © 2001 Elsevier Science B.V. All rights reserved.

Keywords: Reviews; Molecular modeling; Potential energy surfaces; Diastereometric complexes; Molecular simulation; Enantiomer separation

Contents

1. Introduction 418
2. Computational tools and potential energy surfaces 418
3. Approximations, assumptions and an explanation of why differential free energies of binding can be computed accurately 419
4. Methods used for reducing the amount of sampling on potential surfaces 420
5. Chiral stationary phases 421
   5.1. Modeling of type I CSPs 421
      5.1.1. Studies using motif-based searches 421
      5.1.2. Studies using automated search strategies 423
   5.2. Molecular modeling studies of type II CSPs 428
   5.3. Molecular modeling studies of type III CSPs 433
   5.4. Molecular modeling studies of type IV CSPs 437
   5.5. Molecular modeling studies of type V CSPs 439
6. Conclusions 440
Acknowledgements 440
References 440

*Fax: +1-317-274-4701.
E-mail address: lipkowitz@chem.iupui.edu (K.B. Lipkowitz).

0021-9673/01/$ – see front matter © 2001 Elsevier Science B.V. All rights reserved.
PII: S0021-9673(00)00946-8

1. Introduction

Chirality has been thrust to the scientific forefront in several sub-disciplines of the chemical sciences, particularly in organic, biological and pharmaceutical chemistry. Reflecting this are new journals dedicated to the topic of chirality including: *Tetrahedron: Asymmetry*, *Enantiomer*, *Chirality*, and *Molecular Asymmetry*, all of which complement existing journals that are themselves replete with papers on this topic. One area of scientific and technological development that has had a major impact on the way bench chemists go about doing their job is chromatography. Separations scientists have understood for many years that by using a suitable chiral environment, either a stationary phase or a mobile phase additive, one should be able to carry out a direct separation on the chromatographic column without the need of generating diastereomers as intermediates. Enormous advances have been made in such separations in the past decade and nowadays one can purchase a wide range of chromatographic columns and additives for use in planer chromatography, gas-, liquid-, super and subcritical fluid chromatographies and capillary electrophoresis. In spite of these advances a redundant question often heard concerning these chromatographic systems is: ''how do they work''? To address this question a significant number of experimentalists as well as molecular modelers have carried out computational studies on the competing diastereomeric complexes involved in enantiodifferentiation to understand how the intermolecular forces work, in concert, to give rise to chiral separations.

One can now consider molecular modeling as a practical tool for evaluating the complex interactions taking place as analytes migrate through a chromatographic column, providing detailed information at the atomic level, and perhaps from first principles, about how chromatographic systems work. Here we review the applications of computational chemistry in chromatography, illustrating the diversity of computational techniques that have been implemented to rationalize experimental retention orders, and paying special attention to methodologies that have been used to cover fully the potential energy surface. Because of space limitations we restrict our review to those papers where direct interactions between selector and selectand are computed; we unfortunately must omit all of the inventive and insightful regression type models, factorial design and related papers in this review.

2. Computational tools and potential energy surfaces

The computational methods used for atomistic modeling studies have been described in a tutorial manner in this journal in a previous review by the author [1]. Here we assume the reader is familiar with, or has at least heard about, these methods. In particular we assume a basic understanding exists concerning quantum mechanics (QM) and molecular mechanics (MM) calculations, and that you have at least heard about or have a rudimentary knowledge of what molecular dynamics (MD) and Monte Carlo (MC) methods are used for in simulations. A good introductory book covering all of these computational methods has been written by Leach [2], and a review series on the topic of computational chemistry has chapters written as tutorials for the bench chemist [3].

One aspect of molecular modeling that is especially relevant to the modeling of enantioselection in chromatography involves the concept of a potential energy surface (PES). Having knowledge of a molecule's potential energy surface is important because that surface dictates the molecule's shape, its dynamical features and its reactivity. Unfortunately it is difficult to know a priori what the PES looks like with great certainty, except for the simplest of examples. Consider a small molecule with two rotatable bonds. A plot of internal (potential) energy as a function of those two degrees of freedom is given in Fig. 1. While this PES has some apparent symmetry, it is nonetheless fairly complex; imagine, then, what the PES of a molecule, like a cyclodextrin, having tens of rotatable bonds would look like! Fortunately many computational tools allow us to map out such surfaces. In Fig. 1 I depict how these tools are used in an effort to compare and contrast them.

In this diagram the blackened arrow means that a QM or MM geometry optimization (energy minimization) has been done starting from some initial set

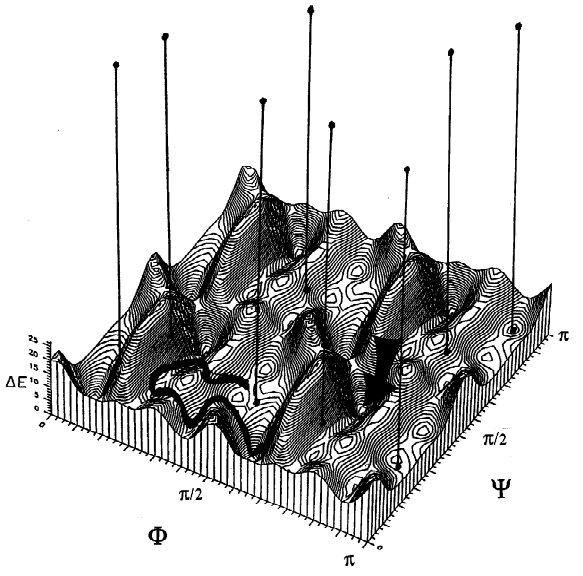

Fig. 1. Part of a complex potential energy surface illustrating the differences between computational methods used to explore such surfaces.

of torsion angles. These energy minimizations usually seek the nearest minimum on the PES so many such minimizations beginning from different starting points are needed to find all the minima. The black dots with lines dropping onto the PES is my representation of what MC calculations involve. Here, randomly selected torsion angles are chosen and the internal energies at those dihedral angles are computed with either a MM potential energy function or a QM Hamiltonian; millions of configurations are thus sampled for statistical thermodynamic averaging. Finally, the black winding line represents the movement over the PES using MD methods. The reason for introducing potential energy surfaces, aside from illustrating the true complexity of their multidimensional nature, is that the biggest error most chemists make when they attempt to calculate enantioselective interactions is to not sample adequately the diastereomeric PESs. Be aware of this issue if you intend to carry out such computations and also when you read the literature concerning such calculations. When done properly, however, an amazing amount of information can be derived, and compelling arguments can be made concerning how stereoselection takes place in both a qualitative and quantitative manner.

3. Approximations, assumptions and an explanation of why differential free energies of binding can be computed accurately

There exist many assumptions and approximations concerning the basic computational methods themselves; these issues are beyond the scope of this review but they are important in their own right and should not be slighted. It is imperative that you have a good working knowledge of these computational techniques or that you consult your local theoretician before becoming too involved in such a project. Also, as in other molecular modeling studies, many scientists will often truncate the size of the receptor or guest, omit buffers, counter-ions and even solvent environments to make the system computationally tractable. This is unfortunate because counter-ions and buffers can influence chromatographic results as can the solvent environment. Indeed, though rare, reversals in enantioselection as a function of solvent composition are known, a good example being the reversal in retention order for a 1,1′-binaphthalene-2,2′-diol on a stationary phase composed of a chiral spirocycle studied by Cuntze and Diederich that will be discussed later in this review (see Ref. [35] for details). At one time the computational methodology and slow computing machinery did not allow one to account for these environmental effects. Nowadays, however, there are fast computers and more importantly there now exist methodology to treat solvent, using either implicit continuum models [4] or explicit models like water [5] as well as pH and pK_a effects [6].

Other approximations related specifically to the calculation of enantioselective binding are also made and we point them out here. First, most scientists do not attempt to compute absolute free energies, but rather determine differential free energies. In all systems where enantioselective binding takes place there exist two competing equilibria:

$$H^R + G^R \rightleftarrows H^R \cdot G^R \quad (1)$$

$$H^R + G^S \rightleftarrows H^R \cdot G^S \quad (2)$$

H refers to the host molecule serving as a selector, G is the guest molecule that is the selectand, and the superscripted R and S are stereochemical descriptors. In both equilibria the binary complexes are often weakly bound, diastereomeric complexes held together by van der Waals forces, hydrogen bonding, charge transfer forces and the like. Most problematic is that the enantiodiscriminating forces are very small compared to the complexation forces, typically by 2–3 orders of magnitude. Hence the computational chemist is faced with the challenging task of computing very small energy differences, often less than 500 cal/mol (1 cal = 4.1868 J).

One could attempt to compute the free energy difference, ΔG, for equilibrium 1, compute the free energy difference for equilibrium 2, and then compare those differences; $\Delta\Delta G$ will thus indicate directly which substrate is more tightly affixed to the host molecule. However, recognize that the left hand side of both equilibria are equivalent; one has the same host molecule, and, by virtue of an enantiomeric relationship, (*R*)-guest = (*S*)-guest because they have the same shapes, same energies and the same extent of solvation in the unbound state. Thus all one needs to do is compute the free energies of the bound state complexes. The differences between the free energies of those complexes, $\Delta\Delta G$, can be used to predict preferential guest binding. This approach is a double difference method first promulgated by DeTar who studied computationally the stereospecificity of chymotrypsin [7]. It is assumed that if the competing binding mechanisms are similar enough, influences of polar effects, solvation effects and entropy differences would cancel, thus making differences in computed energies, either from QM or MM calculations, comparable to differential free energies, $\Delta\Delta G$.

Where this panacea of ''cancellation of errors'' fails is when one inadequately samples the diastereomeric PESs. Merely taking a guest molecule and docking it somehow to a host molecule followed by a simple energy minimization (for D and then for L isomers) is a poor way to compute values for comparison with experiment; what is need are multiple such calculations. Most published papers concerning calculation of enantioselection take advantage of the double difference approach but unfortunately they do not adequately sample enough configurations to make their results meaningful for comparison with experiment. The key question is: how much configurational sampling is needed?

4. Methods used for reducing the amount of sampling on potential surfaces

Most enantioselective binding studies involve binary complexes between one selector and one selectand. Ternary structures are less common except for studies of cyclodextrins where two cyclodextrins can encapsulate one analyte. For capillary electrophoresis this may be a problem for modeling, especially when the stoichiometry is not known, but for lightly loaded chiral stationary phases (CSPs) with immobile cyclodextrins this is not a problem. The first objective of a molecular modeler is to decide where to place the guest in or around the host (and in what relative orientation) before carrying out any other searching on the PES. Knowing where to begin this search is difficult because the PES is not known a priori and because it is so complex. However, methods have been used to help simplify the search. These methods include:

1. Select unambiguous examples to study. In other words, pick a system where there can be only one docking site and one orientation, or for which only a limited number of configurations can exist. This is applicable to studies of protein-based CSPs where the protein has a well-defined binding site.
2. Limit the sampling by using experimental data. Intermolecular NOEs can provide a lot of information about where an analyte binds to a selector, if soluble CSP analogs are available for study, and in some cases it can provide orientational information as well. Alternatively, using crystallographic data can provide a good starting place for docking the pair of molecules.
3. Use ''motif-based docking'' strategies [8]. Here one takes advantage of the known interactions that can take place between two molecules. For example if one molecule has a π-acidic ring and the other a π-basic ring, one would lay one ring over the other to account for the charge transfer complex that will probably occur. Simultaneously one would associate a hydrogen bond donor on one molecule with a hydrogen bond acceptor on

the other and a likewise attempt to match electrostatics between molecules. All of these alignments are good possible beginning points for simulations only; they need not correspond to reality but published examples have shown that this approach, when used judiciously, works quite well and restricts the amount of phase space one needs to sample.

4. Search all of the potential energy surface without making any a priori assumptions; in other words, let the computer do the search for you without any user intervention.

Using one or more of these strategies allows the molecular modeler to generate the initial binary complexes. From this starting point local or even global searches of the PES can be made. All of these techniques have been used to one degree or another in computational studies related to chiral separations in chromatography.

5. Chiral stationary phases

The large number of CSPs developed, tested and marketed present somewhat of a problem for how best to categorize them. Wainer has suggested a classification scheme for high-performance liquid chromatographic (HPLC) CSPs based on the mode of formation of the solute–CSP complex [9]. There are five categories, labeled types I–V, and molecular modeling has been done on most of these. The categories and modes of association are:

Type I. Where solute–CSP complexes are formed by attractive interactions like hydrogen bonding, π–π interactions and dipole stacking as represented by Pirkle-like CSPs.

Type II. Where the solute–CSP complexes are formed by attractive interactions and through the inclusion into a chiral cavity or ravine as represented by some cellulose-based CSPs.

Type III. Where the primary mechanism involves the formation of inclusion complexes as represented by cyclodextrins.

Type IV. Where the solute is part of a diastereomeric metal complex as in chiral ligand exchange chromatography.

Type V. Where the CSP is a protein and the analyte–CSP complexes are based on combinations of hydrophobic and polar interactions.

The major difference between the first three categories, irrespective of the type of intermolecular attractions, is the *extent of inclusion*. Type I has no inclusion complexation, type II has partial inclusion and type III uses inclusion complexation as the ''primary mechanism''. For this review I create a greater line of demarcation between type II and type III phases than did Wainer. Here type III shall be considered to be exclusively guest–host complexes as found in crown ethers, cyclodextrins and related systems, whereas type II uses only partial guest–host complexation.

5.1. Modeling of type I CSPs

To model the interaction between a CSP and an analyte, one must account for: (1) the shapes of the two molecules in the binary complex, (2) the position of the two molecules relative to one another (i.e., the analyte should be at its proper binding site on or around the CSP), and (3) the orientation of the two molecules with respect to each other. This is just a simple way of saying that some sort of ensemble average is needed, where a molecular dynamics protocol must ensure adequate sampling of phase space, or, if using a Monte Carlo strategy, a sufficient number of important configurations must be sampled. The two most frequently used strategies for initial exploration of the diastereomeric PES are: (1) motif-based methods, and (2) full searches using grid-based searching methodologies or either high temperature MD simulation or MC moves to achieve full coverage of the PES. In some cases NOE information from nuclear magnetic resonance (NMR) studies have been used (typically in cyclodextrin and amylose/cellulose oligomers that will be described later in this review).

5.1.1. Studies using motif-based searches

Relatively few motif-based searches have been published. Motif-based search strategies were first developed by Däppen et al. [8] in their computational effort to design new CSPs with enhanced performance. The authors had determined experimentally that the *R*-enantiomer of analyte **1** is bound more tightly to **2**.

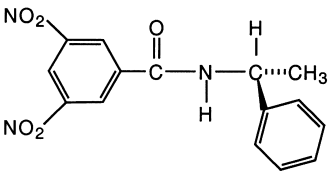

1

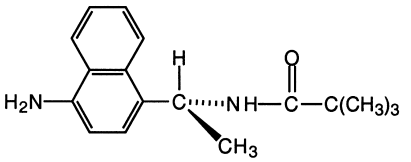

2

Because these authors had determined experimental $\Delta\Delta H$ binding energies they focused their efforts on computing enthalpies rather than free energies. The following steps were recommended as a way to accomplish this. First, carry out a complete conformational analysis of compounds **1** and **2** using MM and/or QM techniques. Second, use those conformers to construct the initial diastereomeric complexes. Last, use some type of a priori classification concerning the possible interactions between parts of the two molecules to reduce the complexity of the problem. Every low-energy conformer of **1** is then combined with every low-energy conformer of **2**, in an orientation such that one or more of the assumed binding motifs is realized.

In their problem three basic binding motifs were considered relevant. These were hydrogen bonds between selector and selectand, dipole stacking of the two amide moieties, and $\pi-\pi$ stacking (charge transfer complexation) between the dinitro π-acid portion of **1** with the π-basic aminonaphthyl ring in **2**. The authors found only three stable conformations of CSP and two stable conformers of analyte, thus giving rise to a relatively small number of initial binary complexes to consider. From this, a small number of possible diastereomeric complexes were generated. Eventually, a Boltzmann weighted average energy for the *RR* complex was computed to be -7.35 kcal/mol at 300 K while that of the corresponding *RS* complex was -5.35 kcal/mol; the 2 kcal/mol energy difference corresponding well with the observed value of 1.22 kcal/mol. Based upon this success the authors then examined various structures to rationalize why one diastereomer is more stable than the other as well as to gain insights about what is needed to improve the stereoselectivity of binding, and finally they delineated an extensive design protocol for the creation of improved CSPs. Another group concerned with the question of how best to sample configurations for statistical averaging was Rogers' group. They had synthesized chiral stationary phases by bonding *tert*-butyloxy carbonyl (BOC) derivatives of amino acids to a butyl spacer on silica and then examined their ability to discriminate between *R*- and *S*-2,2,2-trifluoro-1-(9-anthryl)ethanol, **3**. The modeling involved CSP analog **4** where R = CH_3 (alanine), R = isopropyl (valine), and R′ = different length *n*-alkyl chains.

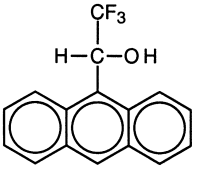

3

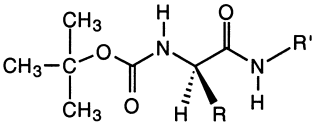

4

Still and Rogers [10] assessed the distribution of conformers for the analyte and the CSP analogs using the MM2 force field. Several docking strategies were employed but only the most stable structures from their conformational analysis were used to form the initial binary complexes. The docking strategies were based on previously determined NMR chemical shifts.

For analyte binding to the BOC-D-alanine-*N*′-*n*-propylamide CSP the *S*-enantiomer was computed by the MM2 force field to be favored by 0.05 kcal/mol, a value that does not agree with experimental retention orders but which is consistent with the small energy difference observed experimentally ($\alpha = 1.02$). When analyte binds to the BOC-D-valine-*N*′-*n*-propylamide CSP the *R*-enantiomer is computed to be favored by 0.18 kcal/mol and this does agree with experiment. The authors concluded that the valine phase would be more effective than the alanine phase and that the *R* analyte would be eluted later than *S* on the valine phase. Both predictions agree with experiment. In spite of this, however, the authors found some inconsistencies with other computational and experimental results. For example, calculation of **4** (with R′ = Me and Et) differed

significantly with those values when a propyl spacer was used; this is a consequence of insufficient sampling and/or not Boltzmann averaging interaction energies. Eventually these authors abandoned the motif-based search strategy for a fully automated search described below.

5.1.2. Studies using automated search strategies

Instead of biasing the results using preconceived notions about binding, Lipkowitz et al. fully automated the search of their potential energy surfaces [11]. The approach developed for sampling the microstates needed for statistical thermodynamic averaging is illustrated in Fig. 2. Here the CSP molecule's center of mass (or any atom) is placed at the origin of a coordinate system. An origin is likewise selected on the analyte and the position of the analyte relative to the CSP is given in polar coordinates.

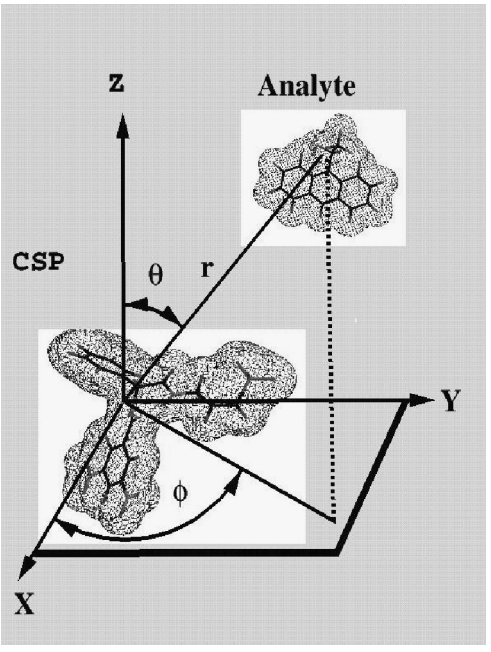

Fig. 2. Position of analyte with respect to chiral stationary phase is given in spherical coordinates, (r, Θ, Φ). r is the distance between arbitrarily selected origins and Θ and Φ describe the latitude and longitude of analyte with respect to CSP. The relative orientations of the two molecules at each latitude and longitude are defined by their Euler angles. Sampling is done as the van der Waals surfaces just touch one another.

At each longitude, Θ, and latitude, Φ, a large number of orientations of the analyte with respect to the CSP are generated. The key to this sampling strategy was to always ensure that the van der Waals surfaces of the two molecules just touched one another (actually the ''touching'' atoms slightly interpenetrated each other somewhat) for each unique orientation generated. Thus, during the sampling, the value of r, the intermolecular separation between selector and selectand, was allowed to vary so that a bulky part of one molecule would not overlap a bulky part of the other molecule. A large number of orientations were sampled at a given value of Θ and Φ. All values of Θ and Φ were then evaluated this way by moving the analyte around the CSP molecule in very small increments so that all minima on the intermolecular potential energy surface were located. In essence what was done was to roll the analyte molecule over the van der Waals surface of the CSP, sampling configurations for the statistical averaging to be carried out.

The rolling motion involved rigid body structures. In this regard the pertinent question was: ''what structures of selector and selectand should be used?'' It was clear that using only the lowest energy conformations (obtained from a conformational analysis) of each molecule would be inappropriate. Just as in the pharmaceutical sciences where it is recognized that the ''bio-active conformation'' of a drug molecule need not be the global minimum, it was felt that the most effective binding shape of the CSP (and/or the analyte) need not be the lowest energy structures either. Indeed, this was found to be the case in several systems that were eventually studied.

Hence, it was necessary to account for all reasonable shapes of CSP as well as of the analyte. This was done by first carrying out a conformational search followed by a Boltzmann weighting of each conformer of CSP and of analyte. If there existed m conformational states of CSP and n conformational states of analyte, $m \times n$ initial binary complexes were constructed, each of which were rolled around one another as described above. For small CSPs like **1** and correspondingly small analytes we typically created several million configurations for the *RR* complex and an equivalent number for the *SR*

complexes, the energies of which were evaluated with a molecular mechanics potential. The averaged energies of these complexes was computed as:

$$\bar{E} = \sum_{h=1}^{1}\sum_{i=1}^{m}\left(\frac{e^{-E_{CSP,h}/kT}}{\sum_{h'=1}^{1} e^{-E_{CSP,h'}/kT}}\right)\left(\frac{e^{-E_{A,i}/kT}}{\sum_{i'=1}^{m} e^{-E_{A,i'}/kT}}\right)\sum_{j=1}^{n} g_{hij}\left(\frac{e^{-\epsilon_{hij}/kT}}{\sum_{j'=1}^{n} e^{-\epsilon_{hij'}/kT}}\right)$$

The terms in parentheses are probabilities. The first term accounts for the probability of finding the CSP in a given conformation, the second term accounts for the probability of finding the analyte in a given conformational state, and the last term is the likelihood of finding the analyte at some position and particular orientation with respect to the CSP. Because all microstates are being sampled this way, their energies and probabilities are known so one can also determine entropies as well as enthalpies of binding. Hence the final energies computed are free energy differences which can be compared to experimental values directly. The influence of differential solvation was also considered [12].

This method works reliably; for all examples that were studied we were able to predict the correct retention order (i.e., the sign of $\Delta\Delta G$ was always correct) and when our differential free energies were converted to separation factors, α, plots of computed versus observed α were linear and usually with high correlation coefficients [11,13–15]. Why does this method work so well, especially when rigid-body sampling motions are involved? The answer is that these transient, diastereomeric complexes are very weakly bound and induced-fit structural changes are relatively insignificant. Moreover, cancellation of errors works in our favor in these systems.

The computational protocol described above was used to calculate differential enthalpies and differential entropies contributing to the free energy differences of the diastereomeric complexes; in all cases the correct retention orders and separation factors agreed well with experiment suggesting the numerical data derived from these simulations were reliable. Based on these successful simulations we answered the following scientific questions: where does the analyte tend to bind around the CSP, and, do both analytes bind to the same or different binding sites? What are the intermolecular forces responsible for complexation? What are the enantiodiscriminating forces, and, are they the same as the forces responsible for complexation? What fragment or fragments of a given CSP are doing most of the work holding the complexes together, and, what fragments are most enantiodiscriminating? Are they the same or different fragments? What conformations of the CSP are most enantiodiscriminating and can this shape be selected and modified to amplify stereoselection? What role does solvent play in selectivity and how does entropy influence selectivity? These and other questions were posited and answered using molecular simulations. What we also found was that many of the existing recognition models being used to rationalized how enantioselection takes place were consonant with our interpretations based exclusively on simulation results with no a priori input from experiment; the advantages we had were that we could provide quantitative measures of the interactions taking place as well as make qualitative arguments.

Other groups have also pursued systematic searches. In the work by Däppen et al. described above [8], the authors also carried out a grid search as follows. Two low-energy conformers are aligned as rigid structures on a six-dimensional grid corresponding to the degrees of freedom of the system. The translational increments were 1 Å and the rotational increments were 24°. The authors implemented CHEM-X to exclude unfavorable lattice regions and generated hundreds of thousands of starting structures. The best 300 structures were selected and then minimized with the CHEM-X force field. The 30 best structures were subjected to QM minimization with all torsion angles and some bond angles allowed to relax. The authors did not find the same low energy diastereomeric complex derived from their motif-based search and decided not to pursue this methodology further, citing the inordinate amount of CPU time required to do the search completely.

In contrast, Still and Rogers abandoned their motif-based search strategy and began developing improved grid searching methods [16]. The system Still and Rogers focused on was the *R*-phenylglycine phase, **5**.

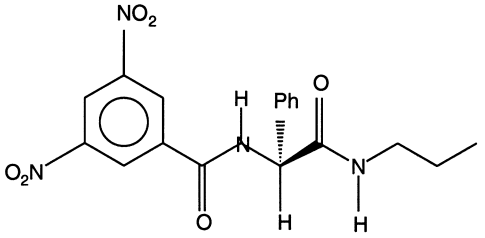

5

Three aminoethanes containing π-basic aryl rings, whose retention orders and separation factors had been determined experimentally, were examined. In all cases the *S*-enantiomer is retained longer on the *R*-CSP. First a conformational analysis using the MM2 force field was carried out. Then, using the most stable structures, the CSP and the analyte were docked using an automated search algorithm. A simplex optimization procedure was used to minimize the nonbonded contact energies of the rigid bodies in the complex. A large number of starting orientations were obtained and a screening process was devised to remove equivalent or near-equivalent structures. Finally, full geometry optimizations were carried out on the docked starting structures that were within 4 kcal/mol of the lowest one. Their method not only predicted the correct elution order for each enantiomeric pair, but also gave reasonable α values. In an ensuing paper [17] they extended the computational study to consider how the dielectric constant of the medium affects the conformer populations, discussed modeling of different size spacer linkages, and, provided far more detail of the structures of the docked species. The authors also demonstrated that relying only on the weighted average enthalpy terms did not always agree with those based on free energies nor with experimental data; as pointed out earlier by Lipkowitz, entropy must be considered.

Other research groups were also carrying out similar work on type I CSPs using a variety of docking strategies and sampling protocols. Aerts, for example, pointed out that Lipkowitz' rigid body approach was only valid in the realm of weak binding; for systems like tartrate ions binding with positively charged diamines there would be significant induced-fit changes that had to be accounted for by full geometry relaxation [18]. Accordingly, Aerts developed an alternative modeling method for prediction of enantioselectivity. His approach for sampling configurations was to use high temperature molecular dynamics trajectories to generate a large number of conformations and orientations of the two molecules in the complex followed by energy minimization of those structures. At 1500 K it is presumed that one can overcome high potential barriers on the PES so that new conformations can be generated while simultaneously creating random orientations of the two molecules with respect to one another. A hard wall constraint was imposed to prevent the two molecules from flying apart during this process. Moreover, it is assumed that both molecules take all possible conformations this way and the results become independent of starting conformation thus providing an advantage in search strategies.

By sampling over the trajectory at regular intervals the author collected a set of configurations, typically around 5000, that were each energy minimized with an empirical force field. These structures were sorted by energy and redundant structures deleted from the list. The probability of finding a D-complex is:

$$p_{\mathrm{D}} = \sum_{j=1}^{N_{\mathrm{D}}} \mathrm{e}^{-E_{\mathrm{D}i}/kT} / \sum_{i=1}^{N} \mathrm{e}^{-E_i/kT} \tag{3}$$

where N_{D} is the number of D complexes. The enantioselectivity is given as the ratio of probabilities:

$$\begin{aligned} \alpha &= [\mathrm{D}]_0/[\mathrm{L}]_0 = N_{\mathrm{D}}/N_{\mathrm{L}} = p_{\mathrm{D}}/p_{\mathrm{L}} \\ &= \sum_i \mathrm{e}^{-E_{\mathrm{D}i}/kT} / \sum_n \mathrm{e}^{-E_{\mathrm{L}n}/kT} \end{aligned} \tag{4}$$

The chromatographic system studied by Aerts is exactly the same evaluated by Däppen et al. [8]. Using 10 000 configurations, Aerts was able to correctly predict the retention order and, depending upon the method used to compute separation factors, obtain fair to excellent results. The conclusions derived from his study refute the hydrogen bonding scheme proposed by Däppen et al. as being important and suggest rather that complexation arises from hydrophobic and dipole stacking forces.

Aerts was not the first to use this kind of search strategy for chromatography. Topiol and co-workers had earlier been studying the chiral recognition of

methyl *N*-(2-naphthyl)alinate with *N*-(3,5-dinitrobenzoyl)leucine *n*-propylamide, a type I CSP analog [19–21]. Sabio and Topiol used room temperature MD trajectories to collect configurations for further energy minimizations with quantum and molecular mechanics [22].

We now highlight the sampling strategies of Gasparrini et al. who created and used various type I CSPs [23]. In particular they have developed phases based on chiral, *trans*-1,2-diaminocyclohexane (DACH), **6**.

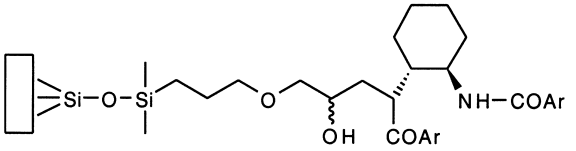

6a Ar = $3,5(NO_2)_2C_6H_3$

6b Ar = $3,5(Cl)_2C_6H_3$

6c Ar = C_6F_5

Extensive analyses of selector–selectand interactions based on NMR studies (of soluble analogs), X-ray crystallography and chromatographic resolutions were used to complement their molecular modeling studies. Gasparrini et al.'s approach is called the Global molecular interaction evaluation (GlobMoline) whose flow chart is outlined in Fig. 3 [24]. Like Lipkowitz and Rogers, Gasparrini considers all conformations of both molecules and computes true free energies from this search strategy. It is to be noted that Gasparrini's simplex optimization of rigid guest with rigid host positions is similar to the work of Rogers and is comparable to Lipkowitz' method using a very fine grid. Eventually, though, the structures located by Gasparrini are fully geometry optimized accounting for induced fit changes of structure. This methodology provides meaningful results when compared to experiment and is currently one of the most robust methods available for computing analyte interactions with type I CSPs.

Bartle et al. proposed a computational method that accounts for the matrix to which these brush-like stationary phases are attached [25]. All prior studies neglected the stationary phase matrix and treated the CSP as if it were freely available to the analyte from all directions. Bartle contends that regions of the CSP near the matrix to which the CSP is grafted are less accessible to the analyte than are other regions. These authors do not explicitly model the matrix, but instead include a penalty function for analyte approach. A schematic of their sampling strategy is presented in Fig. 4. The analyte molecule is moved stepwise around the CSP in a grid-like fashion in an automated and systematic way. In the figure the dotted lines are the loci of points around the CSP. At each point several analyte orientations are considered. Those initial geometries of the binary complex are allowed to relax by minimizing the complex's energy. The authors carried out several thousand minimizations using this sampling strategy and then computed a Boltzmann weighted average energy. Comparison of the weighted averages allows for predicting elution orders and times.

Two examples using these calculations were given. One was the substituted trifluroethanol, binding with a CSP analog previously studied by Lipkowitz, and the second example was the association of an *N*-(3,5-dinitrobenzoyl)-α-methylbenzylamine on a phenyl urea CSP. Their results for the first example are better than those obtained by Lipkowitz and for the latter example are very close to experiment. The authors also addressed how the separation factor, α, is affected by the steric hindrance of the support and found that resolution becomes increasingly difficult as the steric effect increases. Their interpretation of this is that fewer binding sites become available to discriminate between the enantiomers but other interpretations can be envisaged. While the authors implemented only a rudimentary penalty function, their results are good and tend to support their methodology.

Other papers involving the computation of diastereomeric complexes formed on type I CSPs have been published and are cited [26–34]. Note that in Ref. [34] the tripodal, trispeptide selector may be better classified as a type II CSP because it adopts a propeller-like arrangement in apolar to medium polar solvents forming a symmetric, C_3 crown-like structure. This results in inclusion-like complexes as measured experimentally by NMR and other methods, but, this material is used as a stationary phase at high temperatures in gas chromatography and the likelihood of this structure remaining intact under those conditions is questionable. Finally, we point out the study by Cuntze and Diederich [35] who

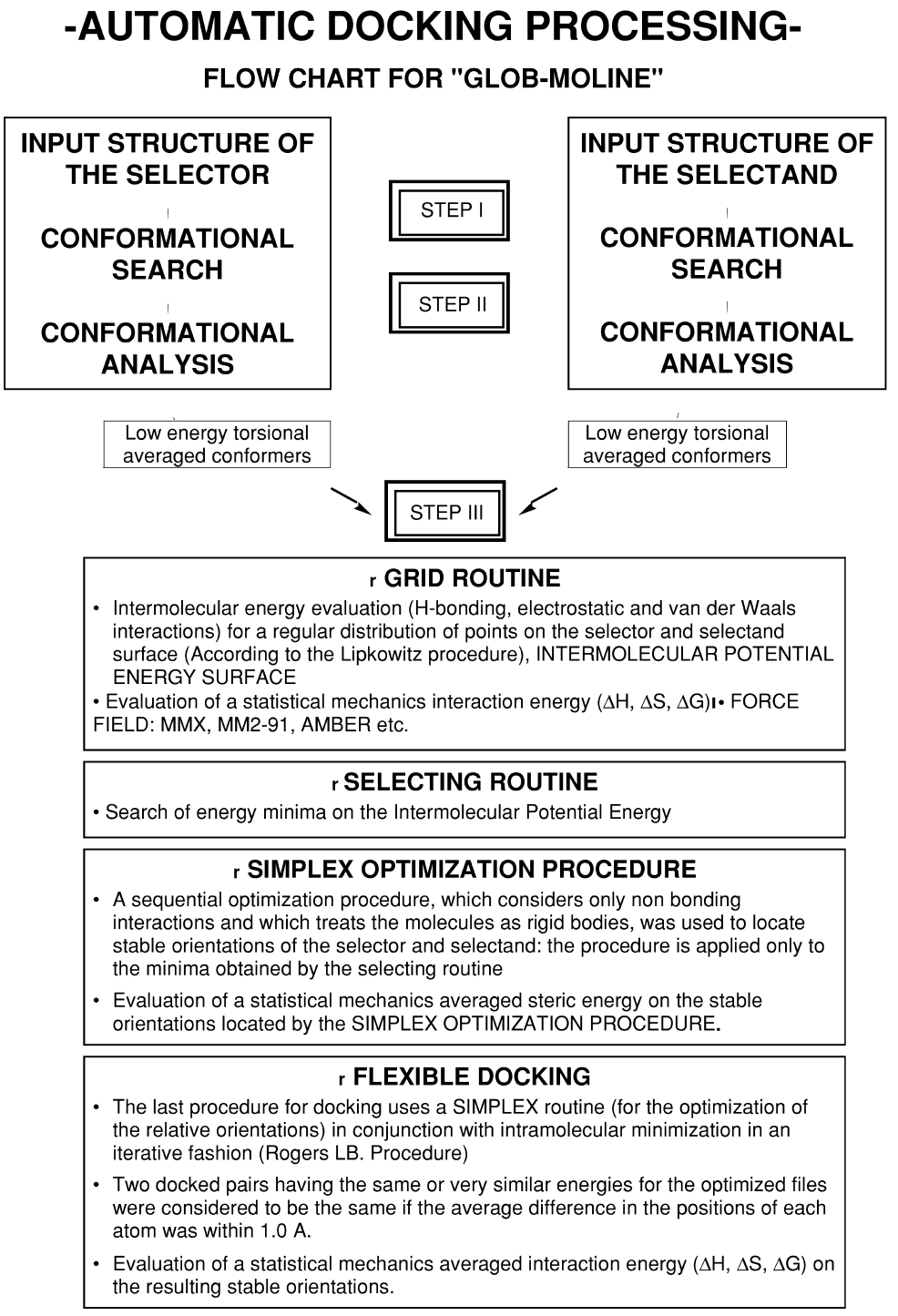

Fig. 3. The Glob-Moline flowchart of Gasparrini et al.

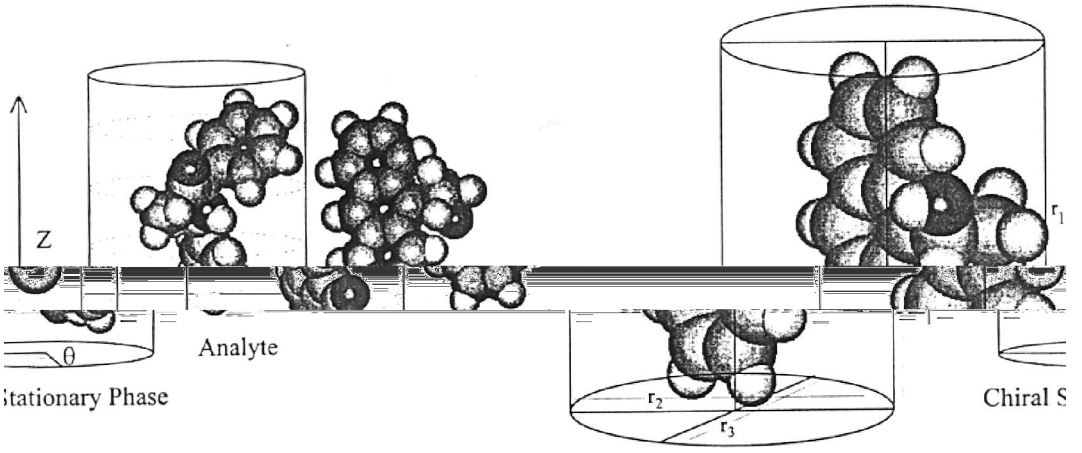

Fig. 4. Left: analyte is moved stepwise around the CSP with a grid that is determined by cylindrical coordinates. Right: dimensions of an imaginary elliptical cylinder surrounding the analyte molecule. Figures provided by K.D. Bartle.

synthesized and immobilized a 9,9′-spiro[9H-fluorene] derivative on silica. This material has clefts into which analytes like 1,1′-binaphthalene-2,2′-diol can be resolved. Their molecular modeling studies clearly show why the longer retained enantiomer is more tightly affixed to the CSP. However, we highlight this study because the separation factor changes and the retention order is inverted when the solvent polarity is changed. This is an especially good system for further study by molecular simulation to better understand the role of solvent in such reversals.

5.2. Molecular modeling studies of type II CSPs

The first scientists to apply atomistic molecular modeling in chiral chromatography were Weinstein et al. Gil-Av had earlier discovered that chiral secondary amides were suitable as chiral stationary phases for gas–liquid chromatography [36]. Most of those amides contain H-bonded stacks of mono-*N*-substituted primary amides with an interstrand spacing of 5 Å, forming the basis for an intercalative model capable of accounting for enantiomer discrimination. Their model, depicted in Fig. 5, assumes

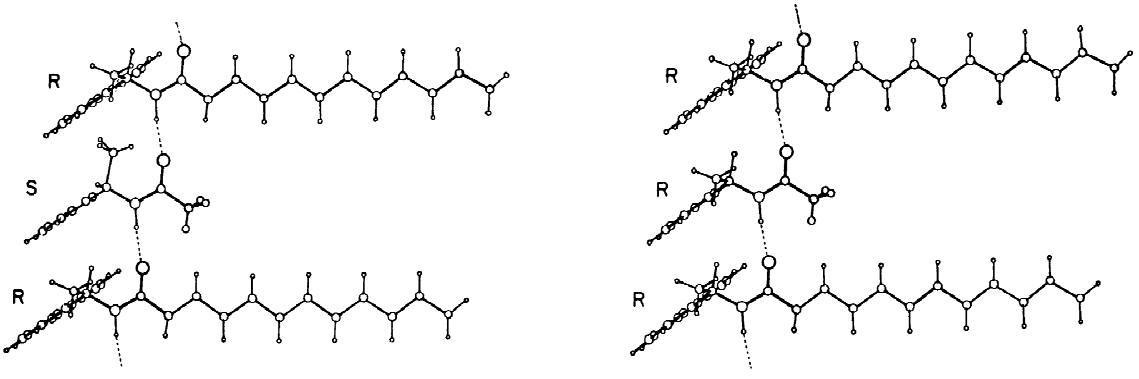

Fig. 5. *N*-Trifluoroacetyl-α-phenylethylamine intercalated into *R*-*N*-lauroyl-α-1-naphthyl)ethylamine. Left: disfavored heterochiral stack. Right: favored homochiral stack.

that bound analytes intercalate within the H-bonded array of the CSP matrix without disrupting that 5 Å, H-bonded motif.

Conformational analysis and packing energies were computed using MM methods. The conformation energy maps gave minimum energy structures in fair agreement with X-ray data. Their chiral recognition model is based on the stacking which fulfills the requirements for linear hydrogen bonds, close packing of aromatic residues and allows for favorable contacts of long R groups [37]. Both analyte molecules can intercalate and maintain the original H-bonding motif but the enantiomer having the same configuration as the CSP fits better than does its antipode (see Fig. 5). This simple intercalation model explains the resolution of enantiomers on the *N*-lauroyl-α-(1-naphthyl)ethylamine CSP and it also explains the reversal of elution orders for α-phenylalkanoic acid amides.

Another example of type II CSPs are those derived from sugar-based polymers like amylose and cellulose. Derivatized celluloses form an especially versatile class of materials that have gained popularity because of their ability to resolve a wide range of drug sized molecules containing many different functional groups. Molecular modeling studies of enantiorecognition by the cellulose triphenylcarbamate CSP has been reported by Camilleri et al. [38]. They carried out separations of oxiracetam, **7**, and two related molecules **8** and **9** on this CSP to assess retention times and separation factors.

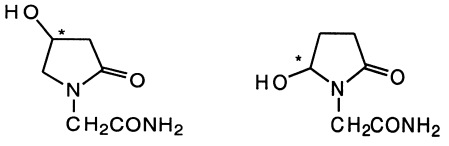

7

8

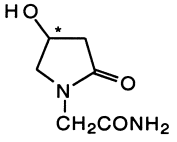

9

For modeling purposes they generated a trisaccharide of β-1,4-linked D-glucoses, end-capped with methyl groups. QM energy minimization resulted in a linear structure with intramolecular H-bonds. The hydroxyls were replaced with phenylcarbamate residues and the resulting trisaccharide was again energy minimized. The phenyl carbamate groups induce a helical twist to the polymer due to steric repulsion of the phenyls but the helicity of the CSP was dismissed as being responsible for chiral recognition. After manual docking of analyte with CSP, energy minimization with molecular mechanics was performed. It was found that only for the *R* isomer of **7** could a viable association exist that would explain why *R* is retained longer than *S*.

Another example of modeling the structure of this type of CSP was presented by Francotte and Wolf [39]. They prepared benzoylcellulose beads, in a pure polymeric form as a sorbent, for the chromatographic resolution of racemic compounds like benzylic alcohols and acetates of aliphatic alcohols and diols. Their experimental results implicated multiple interaction sites to be involved in the complexation. Rationalizing the interaction mechanism required a more systematic investigation of the factors influencing separations and, to address the structural features of the cellulose tribenzoate, they carried out molecular modeling with molecular mechanics. The key question being addressed was: to what extent is the polysaccharide backbone exposed to small molecules when sterically encumbered benzoates are attached?

Representative decameric chain segments were generated by excising the third unit of an energy-minimized hexamer. This excized unit then served as their computational ''monomer.'' This monomer was polymerized, in computero, using the glycosidic bridge angles between the two middle segments to create the polymer backbone. This way the computational artifact of having terminal, end-groups are eliminated. Color-coded molecular graphics displays of the decameric strands in two low-energy conformations revealed the sugar residues are able to interact, at least partially, with small molecules so that the chiral discrimination does not come solely from the benzoyl groups.

Perhaps the most detailed and most comprehensive computational study of chiral analytes binding to type II CSPs comes from Okamoto's laboratory. This group has taken the lead role in developing sugar-based stationary phases and in analyzing chiral

discrimination on polysaccharide derivatives [40,41]. Their molecular modeling involved evaluation of binding energies of ±*trans*-stilbene oxide, a diphenyl epoxide, and ±*trans*-1,2-diphenylcyclopropane (the same system lacking a hydrogen bond binding site) complexing to a cellulose triscarbamate polymer (CTPC) [42]. The reason this particular polymer was selected for study computationally is because it resolves the aforementioned enantiomers with amazing efficiency, but more importantly because this polymer is amenable to NMR spectral analysis using polar solvents.

The polymer was constructed by fully optimizing a triscarbamate monomer containing methoxy groups at the 1- and 4-positions. To do this they used a MM method and the structure that was obtained was, like Francotte and Wolfe, a suitable ''monomer'' for further elaboration. That structure was polymerized, computationally, by linking them to form an octamer with a left-handed, threefold (3/2) helix similar to a CTPC structure previously proposed in the literature based on X-ray fiber diffraction studies. This octamer was then fully geometry optimized and molecular dynamics carried out. From the MD trajectory file was obtained a set of new structures that were energy minimized but no lower energy structures could be found.

Based upon previous experimental work it was hypothesized that the most important adsorbing site for the stilbene oxide involves the N-H hydrogens of the carbamate groups. Accordingly, the authors set up sampling boxes centered around the carbamate's N-H hydrogen. A schematic of both the octamer and the sampling grid are depicted in Fig. 6. Note that a

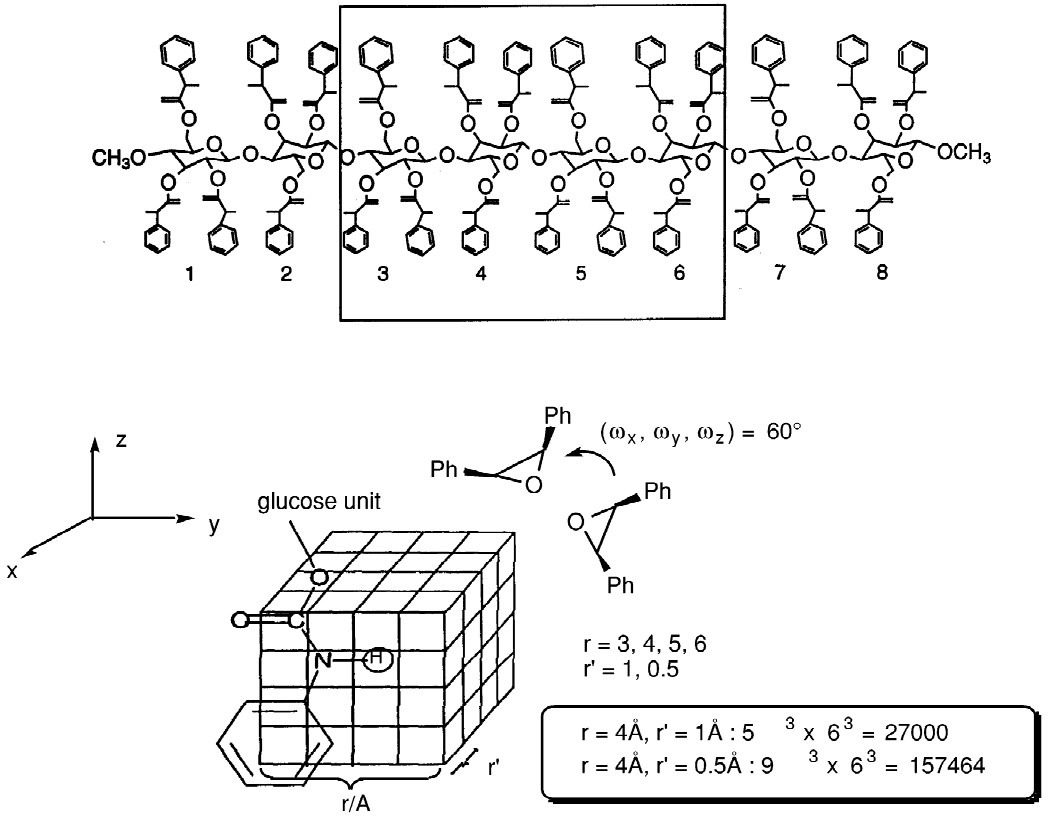

Fig. 6. Top: schematic of cellulose trisphenylcarbamate octamer. Sampling was done within the enclosed box. Bottom: cubic sampling box of dimension *r* and mesh size *r′* in Å. Analyte is rotated in 60° increments about the *x*, *y* and *z* axes at each grid point.

sampling box was set up for all three amides on each monomer, and that only monomers 3–6 were sampled to avoid the influence of the end groups (experimentally these polymers have a degree of polymerization~100). Also note that different grid sizes were used ($r=3$–6 Å) but the grid mesh was initially fixed at 1 Å.

At each grid point the (*R*,*R*)-(+)-epoxide or (*S*,*S*)-(−)-epoxide was rotated in 60° intervals around the *x*, *y*, and *z* axes, individually. The calculations involved a rigid analyte interacting with a rigid CSP. Using this sampling strategy the authors were able to tabulate the minimum interaction energy between analyte and each carbamate moiety on each monomer. Those energies varied substantially, depending on the glucose as well as the position of the carbamate within a particular monomer. Next, a finer grid mesh of 0.5 Å was used and the lowest interaction energies determined. Both grid meshes provided results in agreement with retention orders (the *R*,*R*-enantiomer elutes before the *S*,*S*-enantiomer) but the computed differential interaction energies were substantially overestimated. These energies are not averaged in any way and do not correspond to free energies. Rather, they are presumed to be the global minima of the diastereomeric complexes. Nonetheless the authors were able to find the most probable analyte binding site, which, for the epoxide, is in a chiral groove existing along the main chain of the polymer backbone. Moreover, the authors were able to discern the most important types of interactions including hydrogen bonding to the oxirane ring and π-stacking of carbamates with the analyte phenyl groups. For the diphenylcyclopropane where the hydrogen bonding is absent these researchers found no enantioselective preference from their calculations, and, none was observed experimentally.

Okamoto's group extended this work to a related CSP, cellulose tris(5-fluoro-2-methylphenylcarbamate). Based upon a multifaceted study including chromatography, detailed two-dimensional NMR analyses and molecular modeling, the authors showed that this type II CSP is capable of resolving enantiomers like 1,1′-bi-2-naphthol and 2,2′-dihydroxy-6,6′-dimethylbiphenyl with large separation factors ($\alpha>3$) and that both ^{1}H- and ^{13}C-NMR have large chemical shift changes for the enantiomers. Hence they focused their attention on these kinds of axially disymmetric analytes to address where and how chiral selection takes place [43].

From their HPLC and NMR studies they were able to demonstrate that the *S*-1,1′-bi-2-naphthol, which is more tightly bound to the CSP and accordingly has the longer retention time, binds to a chiral groove on the CSP and is directed toward the glucose *H2* proton. This enantiomer displays several intermolecular NOEs whereas the *R* antipode has none. To further explore the mode of binding Okamoto's group again constructed a left-handed, threefold (3/2) helix. The *R* and *S* analyte structures were derived from a published crystallographic analysis of the racemate. Those crystallographic structures were then fully optimized with a MM force field. The *S*-enantiomer was manually docked into the groove of the CSP in an orientation satisfying all the NMR data and the entire complex was then energy minimized. The structure so derived is illustrated in Fig. 7. The helical chiral cavity along the polymer backbone contains polar carbamate groups inside the groove and hydrophobic aromatic groups outside the groove. From their calculations the authors find that the *S*-enantiomer can simultaneously form two hydrogen bonds to suitably placed polar groups along the chiral groove whereas the *R*-enantiomer can only form a single hydrogen bond. Additionally, the authors were able to rationalize why more bulky systems like 10,10′-dihydroxy-9,9′-biphenanthracene are not resolvable on this particular CSP. While their work entailed mainly molecular mechanics energy minimizations rather than full molecular simulations, the results were particularly useful for discerning where and how enantioselection takes place when axially dissymmetric ligands bind to helical polysaccharides.

A more detailed computational investigation concerning the chiral discrimination mechanism of phenyl carbamate derivatives of cellulose was performed by Yamamoto et al. [44].Two commercially available CSPs were studied: cellulose tris-(phenylcarbamate) (CTPC) and cellulose tris(3,5-dimethylphenylcarbamate) (CDMPC) each of which were interacting with the enantiomers of *trans*-stilbene oxide and with benzoin. The oxirane is separable on the CTPC column having the *S*,*S* antipode retained longer but on the CDMPC column the *R*,*R* isomer is more strongly affixed to the column

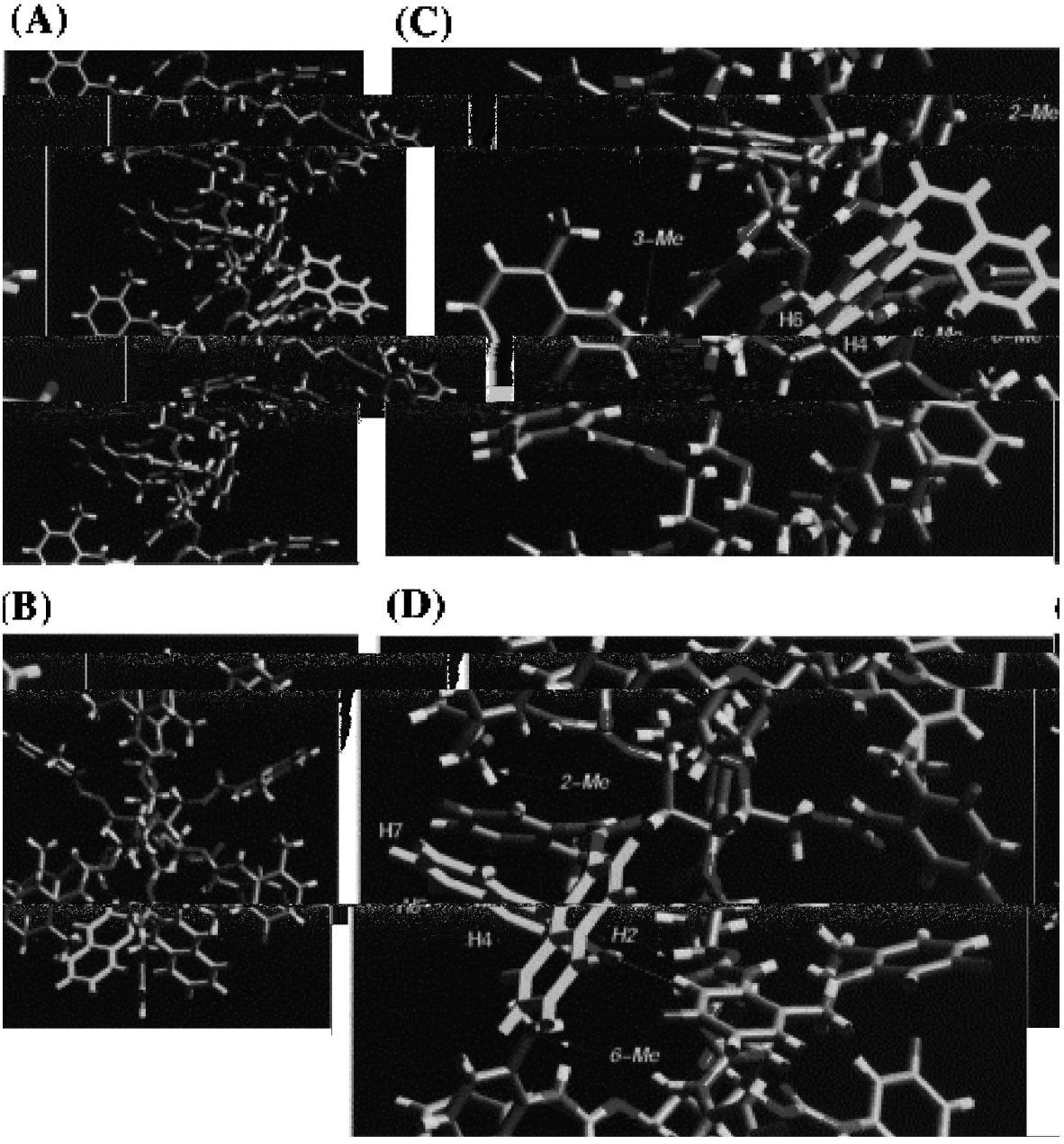

Fig. 7. Complexes of 1,1′-bi-2-naphthol with tris(5-fluoro-2-methylphenylcarbamate) CSP deduced from molecular modeling studies by Okamoto et al. Panels A, B: views parallel and perpendicular the chain axis. Panels C, D: close-up of key interactions of the more tightly bound *S* isomer illustrating key hydrogen bonds (taken with permission from Ref. [43]).

(reversal in enantioselection). The benzoin is separable only on the CDMPC column with the *R* isomer retained longer.

The authors constructed computer models of both CSPs using a somewhat different strategy (albeit very similar) to that described above. A 9-mer was generated and molecular associations with analyte molecules were directed toward the interior units of the oligomer chain to avoid ‘‘end’’ effects. Both polymers are similar in that they are left-handed

helices with polar carbamate groups inside the polymer chain and having hydrophobic groups outside of the chain. Importantly, though, is that the aryl rings of CDMPC are arranged parallel to the helical axis but differently than in CTPC due to the steric hindrance of the methyl groups. It is speculated that this may be responsible for the reversal in enantioselectivity when the two CSPs are compared.

Three computational strategies were used to dock analytes around the CSPs. The first is a deterministic grid search where analyte molecules were placed around the NH and C=O functionality as described above while the other three methods involved analyte placements based on stochastic moves (Monte Carlo) in a polar coordinate system. Most of the structures generated this latter way resulted in the analyte molecules being on the exterior of the polymer surface and not allowing for close contact with the purported NH and C=O binding sites on the interior of the polymer (structures too close to the rigid polymer had very high molecular mechanics energies and were automatically excluded from further consideration). To overcome this problem and to generate diastereomeric complexes where the enantiomers could be generated inside the polymer surface, the authors carried out a series of van der Waals slow-growth calculations where the van der Waals radii of analyte molecules were first reduced in size so that they could approach the interior of the polymer surface and then the radii were alchemically grown back to their standard sizes, incrementally, while the whole system was geometry optimized, beginning from those internally docked positions.

The results from these calculations were in agreement with experiment. Tabulations of intermolecular energy components, energies of interactions with various sites along the polymer chain, and assessments of lowest energy structures as well as averaged structures were presented and discussed. The results indicate that the polar carbamate residues of cellulose derivatives are important adsorbing sites for polar racemates and may play a role in chiral discrimination. It was also speculated that under reverse phase conditions using water eluents, hydrophobic cavities between polymer chains may be important for chiral discrimination. Computational studies in that direction are under way.

Finally, we mention a recent study by O'Brien et al. who evaluated the mechanistic aspects of chiral discrimination on modified cellulose [45]. While the energy minimized complexes they found in their molecular modeling studies were consistent with retention orders, this is an especially interesting system that merits further computational analysis because the separations are enthalpy driven at low temperatures but entropically driven at high temperatures.

5.3. Molecular modeling studies of type III CSPs

Type III CSPs work by forming inclusion complexes. Two main categories of type III CSPs have been studied computationally. These include cyclodextrins (CDs) and their derivatives, and, crown ethers and related non-natural guest–host cavities. In this review we address mainly the cyclodextrins because of their prevalence in capillary electrophoresis as well as in gas and liquid chromatographies but we also provide other examples of some completely synthetic receptors that are used as a type III CSP.

In a series of papers, Armstrong and co-workers used molecular graphics to represent how β-CD separates diastereomers [46] and enantiomers [47,48]. These graphic images were presented in color to highlight similarities and differences of analyte binding, but these studies did not involve complete energy minimizations. Using rigid cyclodextrin, the authors allowed only the important torsion angles and the location of the analyte in the macrocycle to change. The modeling highlighted the importance of the secondary and tertiary hydroxyl groups along the rim of the macrocycle as being responsible for the resolution of enantiomers, and this allowed the authors to rationally design derivatives of CDs to optimize a particular separation. Berthod et al. [49] later devised a scheme useful for attributing individual substituent contributions to chiral recognition. While this method does not allow prediction of an elution order, the substituent constants can be used to make an estimate about enantioselectivity of an unknown analyte simply by adding the energy contributions of the four substituents connected its stereogenic carbon.

The chromatographic behavior of phaclofen, **10**, and its difluoro derivative, **11** along with the diastereomeric monofluoro species **12** and **13** has been studied on acetylated β-CD. In methanol with aque-

ous triethylamine–acetic acid buffer, **10** is not resolved but **11** is

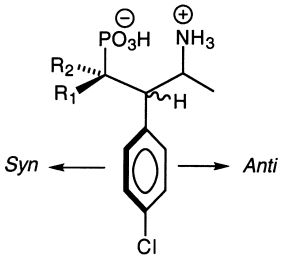

10 $R_1 = R_2 = H$
11 $R_1 = R_2 = F$
12 $R_1 = H, R_2 = F$
13 $R_1 = F, R_2 = H$

with $\alpha = 1.11$. Also, compound **13** is resolved but not **12**. A theoretical model for this behavior, described in terms of the asymmetry in the π-facial molecular electrostatic potentials of the phenyl ring, was proposed by Camilleri et al. [50]. The electrostatic potentials on the *syn* and *anti* faces of the aryl ring were determined; those analytes with bigger electrostatic differences between *syn* and *anti* faces appear to correlate with separations but precisely how this electrostatic asymmetry works was not divulged.

Our interest in chiral discrimination by type III CSPs began when we learned that amino acids like tryptophan could be resolved on a cyclodextrin CSP. We first carried out NMR studies using the same solvent medium as was used for the chromatography experiments and we demonstrated that the tryptophan is indeed included within the macrocycle under chromatographic conditions [51]. Moreover, based upon NOE intensities of key protons of guest with those of host, we had some a priori knowledge about the geometry of the complexes that we used for our simulations. We felt that the rigid body approach described earlier was not tenable for these host molecules because they are very flexible and are prone to induced-fit structural changes. Hence molecular dynamics calculations, which account well for this flexibility, were carried out using the same explicit solvents as in the chromatographic and NMR studies. Using the CHARMM force field for molecular dynamics, our simulations reproduced the correct retention order and separation factor from the chromatography experiments, and, our simulation results also agreed with both intermolecular and intramolecular NOE observations from our NMR experiments.

Because intermolecular hydrogen bonding was considered to be important, we evaluated the number and kinds of intermolecular H-bonds between guest and host. We found that not only does the more retained *R*-enantiomer form a greater number of H-bonds than does *S*, but also that these H-bonds are usually simultaneous, multiple-contact H-bonds between guest and host. A cartoon summarizing our findings in this regard is depicted in Fig. 8.

Three key features emerge from this figure. First, both complexes are highly localized on the interior of the CD with *R* binding to one side of the macrocycle and *S* to the other. Second, the *R*-enantiomer forms nearly twice as many intermolecular H-bonds as does *S* and, as pointed out above, they are of the multiple-contact type. Third, the hydrogen bonding occurs primarily from tryptophan's carboxylate and indole N-H but not the ammonium group. Based on this we confirmed an earlier recognition model but pointed out that a high degree of localization is tantamount to a tight fit in the CD cavity. These studies were followed by an assessment of mandelic acid binding to β-cyclodextrin using chromatography, NMR spectroscopy and molecular dy-

Fig. 8. Graphical representation of the intermolecular hydrogen bonds of (*R*)- and (*S*)-tryptophan with α-cyclodextrin. The large circle represents the macrocyclic host. The small black dots on that circle are the acetal linker oxygens, and the lines attached to the circle represent the unidirectional C_2 and C_3 hydroxyl groups. The cross-hatching indicates the atoms or groups of atoms on the tryptophan that are forming the intermolecular hydrogen bonds. The size of the crosshatched circle corresponds to the number of hydrogen bonds formed during the simulation. The centers of the cross-hatched circles are placed at the mean positions of the hydrogen bond contacts. There exist 2662 and 1307 hydrogen bonding interactions for the *R* and *S* analytes, respectively.

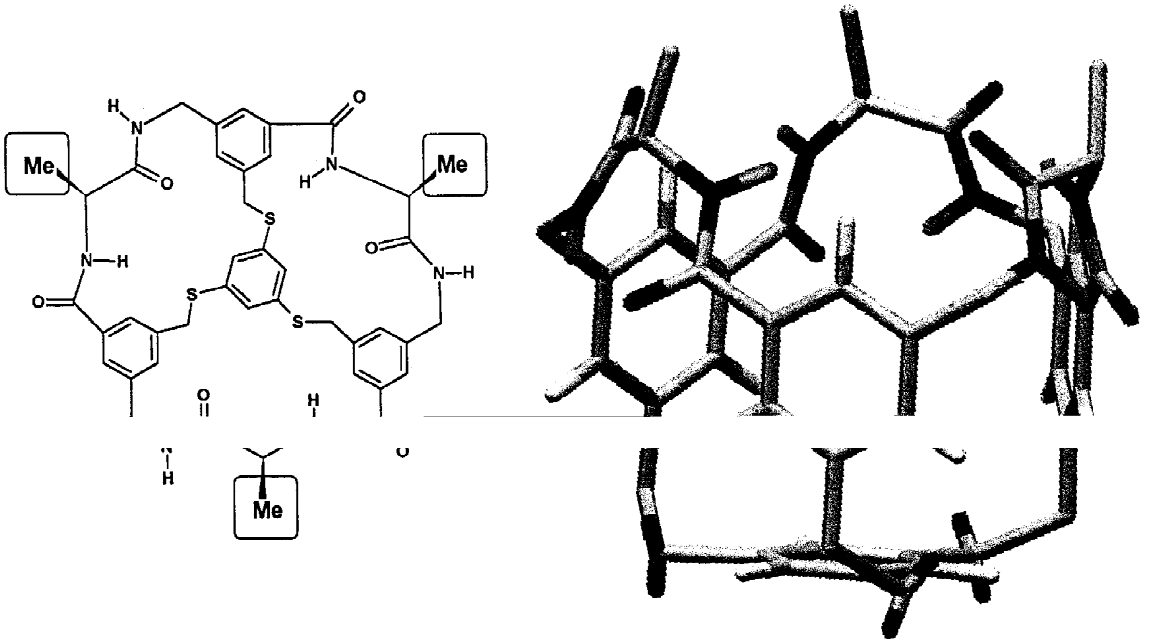

Fig. 10. Left: schematic of Hong et al.'s C_3 symmetric L-tyrosyl macrocyclic CSP with tyrosyl side chains replaced by methyl groups. Right: lowest energy conformer of host molecule illustrating the depth of its chiral cavity.

exchange chromatography (CLEC). To our knowledge there exists only a single publication where chromatography and molecular modeling were used together, viz., a recent paper by Chilmonczyk et al. [84]. In this study a CSP containing L-hydroxyproline was chemically bound by a glycidoxypropyl spacer chain to silica for the resolution of α-hydroxy acids. The elution order was interpreted in terms of an existing recognition model but the structures of the ternary complexes were determined quantum mechanically. In that regard a semi-empirical, Hartree Fock method and a density function method were used. Three types of complexes were considered and the relative stability of each complex was found to depend upon how the copper metal site is coordinated (in addition to the influence of coordinating water). Unfortunately no consistent agreement between experiment and theory was found. In another paper a molecular mechanics study on ligand-exchange reactions of an optically pure Ni(II) complex was carried out by Bernhardt et al. but no chromatography was done in their assessment of complex stability [85].

There do exist molecular modeling studies of inorganic coordination complexes that have been used as chiral mobile phase additives for separations, and atomistic modeling in chiral ion-pair chromatography. Bazylak [86,87] compared the resolution of underivatized primary and secondary amino alcohols by reverse phase HPLC. He used helically distorted nickel(II) Schiff base chelates as a mobile phase additive. These coordination complexes do not work like traditional ligand exchange chelates because their structures remain intact during association with analytes. The coordinating bonds between the nickel and Schiff-base ligand are neither broken nor formed, and the coordinatively unsaturated nickel(II) only has specific steric and electrostatic interactions with the two analytes. No energy calculations were done. Instead, least-squares superpositions of analyte with chelating reagent were depicted showing where the author believes negatively charged amine groups associate with the metal and how other interactions like π-stacking with the chelate rings induce chiral discrimination.

Another report on ion-pair chromatography, where computed molecular descriptors from molecular modeling were nicely correlated with experimental

separation factors, was published by Karlsson et al. [88]. They examined factors responsible for separation of aminotetralins on achiral stationary phases in the presence of the chiral additive *N*-benzyloxycarbonylglycyl-L-proline (L-ZGP), a protected peptide derivative.

Using molecular mechanics these authors first determine the distribution of conformational states accessible to the analytes and then evaluated the preferred conformations of L-ZGP in the neutral and ionic forms. Then the authors brought these components together to form the various diastereomeric complexes. Their strategy was to implement a flexible docking scheme because it was felt that both molecules of the complex may change their conformations during association.

The authors found typically 40 conformations within 3 kcal/mol of the global minimum for their analytes and 243 low-energy conformations for L-ZPG, requiring ca. 40×243 docking combinations, each having a large number of orientations and positions with respect to one another. Thus a computer-aided docking protocol was used in addition to manual docking. Following the methodologies of Lipkowitz et al. [11], Still and Rogers [10] and Gasparrini et al. [24] described in an earlier section, the authors decided not to use only the lowest energy structures, but rather, all their structures to derive averaged energies and averaged properties for comparison to experiment. The best molecular descriptor they found correlating theory with experiment is the averaged nonpolar unsaturated surface area of the complex. In another paper they extended their studies [89] where similar conclusions were derived. The reported deficiencies in molecular modeling studies of type IV CSPs may sometimes be related to bad parameterization of force fields or of semiempirical Hamiltonians for inorganic centers due to lack of experimental data. This is an area of fruitful future work.

5.5. Molecular modeling studies of type V CSPs

Type V CSPs are protein phases. Most of the molecular modeling done on these CSPs involve regression methods that we have excluded from this review because of space constraints. The reason scientists have carried out such modeling is mainly because details about the shape of the protein binding site are not known at an atomic level. Instead, a series of analytes are separated and molecular descriptors of those analytes are correlated with the ability of the protein to resolve them. Only one example has appeared in the literature where information from the Protein Database (PDB) has been used to serve as a beginning point for molecular modeling of a protein CSP.

Pinkerton et al. [90] addressed the chiral discrimination of stationary phases made from intact and fragments of turkey ovomucoid. Turkey ovomucoid was selected for this study because previous NMR assignments of its third domain had been published. A commercially available CSP made of this protein exists. The authors isolated several protein domains that were subsequently covalently attached to silica gel and used to examine enantioselectivity for a large number of test racemates. The authors generated chromatographic columns containing the following materials: whole turkey ovomucoid (OMTKY), a combination of first and second domains (OMTKY[1+2]), the second domain (OMTKY2), the glycosylated third domain (OMTKY3S) and the nonglycosylated third domain (OMTKY3). The third domain displayed the best chiral recognition for benzodiazepines and profens.

Extensive NMR titration studies together with NOESY results provided analyte association constants and information about the binding sites on the third domain. Their molecular modeling began by extracting the atomic coordinates of silver pheasant ovomucoid third domain from the PDB and converting Met 18 to Leu, thus generating OMTKY3. Two analytes were considered: pranoprofen and a related heterocycle designated as U-80,413. These analytes were geometry optimized and then bound to the protein using a program called Autodock. This docking program allowed each enantiomer to search the surface of the OMTKY3 for low energy binding orientations while keeping both the selector and selectand rigid. Each docking was scored by summing the van der Waals and electrostatic interactions of the selector with the selectand. Typically about 6500 orientations were generated for each enantiomer and the best 200 were energy minimized, allowing the analyte to fully relax but keeping the protein rigid. Only 100 of the best structures (lowest

energy) were kept as a working set. The authors located potential binding sites on the protein this way and found their results to be consistent with independent NMR results. Then, using the NMR results, they selected the six best docking orientations for each enantiomer in each set.

From their computations they found: (1) the *R*-enantiomer is bound closer to the protein than is *S*; (2) the *R* analytes typically have lower binding energies; (3) two major binding domains exist, one on each side of the protein, such that analytes cannot bind simultaneously to both sites. Of these two sites one was found to be comprised of mainly hydrophobic amino acids. Computed binding energies at this region are generally of higher energy than at the other site, and, nonspecific binding orientations lead to a lack of chiral discrimination in this site. For the lower energy binding domain the authors enumerated the similarities and the differences of enantiomer binding. All of their computed results were consistent with experimental facts but the authors indicated that a chiral recognition mechanism could not yet be described without ambiguity.

6. Conclusions

A review covering atomistic molecular modeling studies related to chromatographic resolution of enantiomers has been presented. Included in this review are publications where the competing diastereomeric complexes have been computed directly; omitted are many papers where factorial design strategies, QSAR (Quantitative Structure Activity Relationships), and related regression methods have been used to help explain the origins of enantioselectivity. Type I–V CSPs have been covered in addition to chiral additives used for ion-pair chromatography and capillary electrophoresis. An effort was made to highlight the need to adequately sample the potential energy surfaces of the competing diastereomeric complexes (Fig. 1). In this regard we find that the most frequently used methods to help reduce the amount of configurational space needed to be search involves: (1) the use of experimental data like nuclear Overhauser enhancements from NMR spectroscopy, or (2) the use of motif-based docking strategies to assist in generating the binary complexes. Even with this information care must be taken to ensure that the important regions of the diastereomeric potential energy surfaces have been sampled adequately, and that a statistical averaging of results has been performed. Nowadays, because of fast computers and large disk space, many computational chemists are not making any a priori assumptions at all, and letting the computer do full searches for them without any user bias. Because double differences are being computed a cancellation of errors often provides good results for comparison with experiment. When agreement with experiment exists, one can extract valuable information from the simulation concerning the atom–atom interactions leading to chiral discrimination. When done properly these computational methods can be a valuable adjunct to existing experiment as well as being predictive in their own right.

Acknowledgements

The author's work described herein was carried out with grants from the National Science Foundation (CHE-998288) and the Petroleum Research Fund administered by the American Chemical Society (≠35172-AC).

References

[1] K.B. Lipkowitz, J. Chromatogr. A 694 (1995) 15.
[2] A.R. Leach, Molecular Modeling – Principles and Applications, Addison Wesley Longman, Essex, 1996.
[3] K.B. Lipkowitz, D. Boyd (Eds.), Reviews in Computational Chemistry, Vols. 1–16, Wiley–VCH, New York, 1990–2000.
[4] C.J. Cramer, D.G. Truhlar, in: K.B. Lipkowitz, D.B. Boyd (Eds.), Reviews in Computational Chemistry, Vol. 6, VCH, New York, 1995, p. 1, Chapter 1.
[5] A. Walqvist, R.D. Mountain, in: K.B. Lipkowitz, D.B. Boyd (Eds.), Reviews in Computational Chemistry, Vol. 13, Wiley–VCH, New York, 1999, p. 183, Chapter 4.
[6] J.M. Briggs, J. Antosiewicz, in: K.B. Lipkowitz, D.B. Boyd (Eds.), Reviews in Computational Chemistry, Vol. 6, Wiley–VCH, New York, 1999, p. 249, Chapter 5.
[7] D.F. De Tar, Biochemistry 20 (1981) 1730.
[8] R. Däppen, H.R. Karfunkel, F.J.J. Leusen, J. Comput. Chem. 11 (1990) 181.
[9] I.W. Wainer, Trends Anal. Chem. 6 (1987) 125.
[10] M.G. Still, L.B. Rogers, Talanta 36 (1989) 35.

[11] K.B. Lipkowitz, D.A. Demeter, R. Zegarra, R. Larter, T. Darden, J. Am. Chem. Soc. 110 (1988) 3446.
[12] K.B. Lipkowitz, B. Baker, R. Larter, J. Am. Chem. Soc. 111 (1989) 7750.
[13] K.B. Lipkowitz, B. Baker, R. Zegarra, J. Comput. Chem. 10 (1989) 718.
[14] K.B. Lipkowitz, B. Baker, Anal. Chem. 62 (1990) 770.
[15] K.B. Lipkowitz, S. Antell, B. Baker, J. Org. Chem. 54 (1990) 5449.
[16] M.G. Still, L.B. Rogers, J. Comput. Chem. 11 (1990) 242.
[17] M.G. Still, L.B. Rogers, Talanta 37 (1990) 599.
[18] J. Aerts, J. Comput. Chem. 16 (1995) 914.
[19] S. Topiol, M. Sabio, J. Moroz, W.B. Caldwell, J. Am. Chem. Soc. 110 (1988) 8367.
[20] S. Topiol, M. Sabio, J. Chromatogr. 461 (1989) 129.
[21] M. Sabio, S. Topiol, Int. J. Quantum Chem. 36 (1989) 313.
[22] M. Sabio, S. Topiol, Chirality 3 (1991) 56.
[23] F. Gasparrini, L. Lunazzi, D. Misiti, C. Villani, Acc. Chem. Res. 28 (1995) 163.
[24] F. Gasparrini, M. Pierini, S. Alcaro, S. Mecucci, O. Incani, presented at the 8th International Symposium on Chiral Discrimination, Edinburgh, 2 July 1996.
[25] A.M. Edge, D.M. Heaton, K.D. Bartle, A.A. Clifford, P. Myers, Chromatographia 41 (1995) 161.
[26] U. Norinder, E.G. Sundholm, J. Liq. Chromatogr. 10 (1987) 2825.
[27] U. Norinder, E.G. Sundholm, in: D. Stevenson, D. Wilson (Eds.), Chiral Separations, Plenum Press, New York, 1988, p. 127.
[28] G. Krüger, J. Grötzinger, H. Berndt, J. Chromatogr. 397 (1987) 223.
[29] R. Däppen, H.R. Karfunkel, F.J.J. Leusen, J. Chromatogr. 469 (1989) 101.
[30] T. Hanai, H. Hatano, N. Nimura, T. Kinoshita, J. Liq. Chromatogr. 16 (1993) 801.
[31] P. Camilleri, D.S. Eggleston, H.S. Rzepa, M.L. Webb, J. Chem. Soc., Chem. Commun. (1994) 1135.
[32] H.Y. Aboul-Enein, V. Serignese, Chirality 7 (1995) 158.
[33] C. del Campo, E.F. Llama, J.V. Sinisterra, Tetrahedron: Asymmetry 7 (1996) 2627.
[34] F. Betschinger, J. Libman, C.E. Felder, A. Shanzer, Chirality 10 (1998) 396.
[35] J. Cuntze, F. Diederich, Helv. Chim. Acta 80 (1997) 897.
[36] S. Weinstein, B. Feibush, E. Gil-Av, J. Chromatogr. 126 (1975) 97.
[37] S. Weinstein, L. Leiserowitz, E. Gil-Av, J. Am. Chem. Soc. 102 (1980) 2768.
[38] P. Camilleri, J.A. Murphy, M.R. Saunders, C.J. Thorpe, J. Comput.-Aided Molec. Design 5 (1991) 277.
[39] E. Francotte, R.M. Wolf, Chirality 3 (1991) 43.
[40] E. Yashima, Y. Okamoto, Bull. Soc. Chem. Jpn. 68 (1995) 3289.
[41] Y. Okamoto, E. Yashima, Angew. Chem. Int. Ed. Engl. 37 (1998) 1021.
[42] E. Yashima, M. Yamada, Y. Kaida, Y. Okamoto, J. Chromatogr. A 694 (1995) 347.
[43] E. Yashima, C. Yamamoto, Y. Okamoto, J. Am. Chem. Soc. 118 (1996) 4036.
[44] C. Yamamoto, E. Yashima, Y. Okamoto, Bull. Chem. Soc. Jpn. 72 (1999) 1815.
[45] T. O'Brien, L. Crocker, K. Thompson, P.H. Toma, D.A. Conlon, B. Feibush, C. Moeder, G. Bicker, N. Grinberg, Anal. Chem. 69 (1997) 1999.
[46] R.D. Armstrong, T.J. Ward, N. Pattabiraman, C. Benz, D.W. Armstrong, J. Chromatogr. 414 (1987) 192.
[47] R.D. Armstrong, in: W.L. Hinze, D.W. Armstrong (Eds.), Ordered Media in Chemical Separations, ACS Symposium Series, No. 342, American Chemical Society, Washington, DC, 1987, Chapter 16.
[48] D.W. Armstrong, T.J. Ward, R.D. Armstrong, T.E. Beesley, Science 232 (1986) 1132.
[49] A. Berthod, S.-C. Chang, D.W. Armstrong, Anal. Chem. 64 (1992) 395.
[50] P. Camilleri, A.J. Edwards, H.S. Rzepa, S.M. Green, J. Chem. Soc., Chem. Commun. (1992) 1122.
[51] K.B. Lipkowitz, S. Raghothama, J.-A. Yang, J. Am. Chem. Soc. 114 (1992) 1554.
[52] K.B. Lipkowitz, C.M. Stoehr, Chirality 8 (1996) 341.
[53] J.E.H. Köhler, M. Hohla, M. Richters, W.A. König, Angew. Chem. 104 (1992) 362.
[54] J.E.H. Köhler, M. Hohla, M. Richters, W.A. König, Angew. Chem., Int. Ed. Engl. 31 (1992) 319.
[55] J.E.H. Köhler, M. Hohla, M. Richters, W.A. König, Chem. Ber. 127 (1994) 119.
[56] N. Koen de Vries, B. Coussens, R.J. Meier, J. High Resolut. Chromatogr. 15 (1992) 499.
[57] F. Kobor, K. Angermund, G. Schomburg, J. High Resolut. Chromatogr. 16 (1993) 299.
[58] D.R. Black, C.G. Parker, S.S. Zimmerman, M.L. Lee, J. Comput. Chem. 17 (1996) 931.
[59] K.B. Lipkowitz, G. Pearl, B. Coner, M.A. Peterson, J. Am. Chem. Soc. 119 (1997) 600.
[60] K.B. Lipkowitz, B. Coner, M.A. Peterson, A. Morreale, J. Phys. Org. Chem. 10 (1997) 311.
[61] K.B. Lipkowitz, B. Coner, M.A. Peterson, J. Am. Chem. Soc. 119 (1997) 11269.
[62] K.B. Lipkowitz, B. Coner, M.A. Peterson, A. Morreale, J. Shackelford, J. Org. Chem. 63 (1998) 732.
[63] V. Schurig, H.-P. Nowotny, Angew. Chem. Int. Ed. Engl. 29 (1990) 939.
[64] D.G. Durham, H. Liang, Chirality 6 (1994) 239.
[65] P. Camilleri, C.A. Reid, D.T. Manallack, Chromatographia 38 (1994) 771.
[66] C.L. Copper, J.B. Davis, R.O. Cole, M.J. Sepaniak, Electrophoresis 15 (1994) 785.
[67] Y. Kuroda, Y. Suzuki, J. He, T. Kawabata, A. Shibukawa, H. Wada, H. Fujima, Y. Go-oh, E. Imai, T. Nakagawa, J. Chem. Soc., Perkin Trans. 2 (1995) 1749.
[68] E. Tesarová, M. Gilar, P. Hobza, M. Kabelác, Z. Deyl, E. Smolková-Keulemansová, J. High Resolut. Chromatogr. 18 (1995) 597.
[69] K. Kano, K. Minami, K. Horiguchi, T. Ishimura, M. Kodera, J. Chromatogr. A 694 (1995) 307.
[70] R. Reinhardt, M. Richter, P.P. Mager, P. Hennig, W. Engewald, Chromatographia 43 (1996) 187.

[71] S. Topiol, M. Sabio, Enantiomer 1 (1996) 251.
[72] D.G. Durham, Chirality 8 (1996) 58.
[73] P.K. Owens, A.F. Fell, M.W. Coleman, J.C. Berridge, Chirality 8 (1996) 466.
[74] P. Cozzini, P. Domiano, P.C. Musini, G. Palla, E. Zanardi, J. Inclusion Phenom. Molec. Recognit. Chem. 26 (1996) 295.
[75] K. Kano, Y. Kato, M. Kodera, J. Chem. Soc., Perkin Trans. 2 (1996) 1211.
[76] J. Liu, H. Coffey, D.J. Detlefsen, Y. Li, M.S. Lee, J. Chromatogr. A 763 (1997) 261.
[77] X. Zhu, B. Lin, U. Epperlein, B. Koppenhoefer, Chirality 11 (1999) 56.
[78] K. Lipkowitz, Chem. Rev. 98 (1998) 1829.
[79] J.-I. Hong, S.K. Namgoong, A. Bernardi, W.C. Still, J. Am. Chem. Soc. 113 (1991) 5111.
[80] F. Gasparrini, D. Misiti, C. Villani, A. Borchardt, M.T. Burger, W.C. Still, J. Org. Chem. 60 (1995) 4314.
[81] S. Alcaro, F. Gasparrini, O. Incani, S. Mecucci, D. Misiti, M. Pierini, C. Villani, J. Comput. Chem. 21 (2000) 515.
[82] J. Bradshaw, R.M. Izatt, J.J. Christensen, K.E. Krakowiak, B.J. Tarbet, R.L. Bruening, J. Inclusion Phenom. Molec. Recognit. Chem. 7 (1989) 127.
[83] R.J. Pieters, J. Cuntze, M. Bonnet, F. Diederich, J. Chem. Soc., Perkin Trans. 2 (1997) 1891.
[84] Z. Chilmonczyk, H. Ksycinska, J. Cybulski, M. Rydzewski, A. Les, Chirality 10 (1998) 821.
[85] P.V. Bernhardt, P. Comba, T.W. Hambley, I. Sóvágó, K. Varnágy, J. Chem. Soc., Dalton Trans. (1993) 2023.
[86] G. Bazylak, J. Chromatogr. A 665 (1994) 75.
[87] G. Bazylak, J. Chromatogr. A 668 (1994) 519.
[88] A. Karlsson, K. Luthman, C. Pettersson, U. Hacksell, Acta Chem. Scand. 47 (1993) 469.
[89] K. Luthman, A.V. Jensen, U. Hacksell, A. Karlsson, C. Pettersson, J. Chromatogr. A 666 (1994) 527.
[90] T.C. Pinkerton, W.J. Howe, E.L. Ulrich, J.P. Comisky, J. Haginaka, T. Murashima, W.F. Walkenhorst, W.M. Westler, J.L. Markley, Anal. Chem. 67 (1995) 2354.